Supporting Information

Microfluidic device for One-step Detection of breast cancer-derived Exosomal mRNA in blood using Signal-amplifiable 3D Nanostructure

Jaewoo Lim [1,2], Byunghoon Kang [1], Hye Young Son [4,5], Byeonggeol Mun [3], Yong-Min Huh [4,6], Hyun Wook Rho [4], Taejoon Kang[1], Jeong Moon[1,7], Jae-Jong Lee[8], Seung Beom Seo [1,9], Soojin Jang [1,2], Seong Uk Son [1], Juyeon Jung[1,2], Seungjoo Haam[3,], Eun-Kyung Lim [1,2,*]*

[1]Bionanotechnology Research Center, Korea Research Institute of Bioscience and Biotechnology (KRIBB), 125 Gwahak-ro, Yuseong-gu, Daejeon, 34141, Republic of Korea

[2]Department of Nanobiotechnology, KRIBB School of Biotechnology, University of Science and Technology (UST), 125 Gwahak-ro, Yuseong-gu, Daejeon, 34113, Republic of Korea

[3]Department of Chemical & Biomolecular Engineering, College of Engineering, Yonsei University, 50 Yonsei-ro, Seodaemun-gu, Seoul 03722, Republic of Korea

[4]Department of Radiology, College of Medicine, Yonsei University, 50-1 Yonsei-ro, Seodaemun-gu, Seoul, 03772, Republic of Korea

[5]YUHS-KRIBB Medical Convergence Research Institute, 50-1 Yonsei-ro, Seodaemun-gu, Seoul, 03722, Republic of Korea

[6]Severance Biomedical Science Institute, College of Medicine, Yonsei University, 50-1 Yonsei-ro, Seodaemun-gu Seoul, 03722, Republic of Korea

[7]Department of Chemical and Biomolecular Engineering (BK 21+ Program), KAIST, 291 Daehak-ro, Yuseong-gu, Daejeon, 34141, Republic of Korea

[8]Department of Nano Manufacturing Technology, Korea Institute of Machinery and Materials (KIMM), 156 Gajeongbuk-ro, Yuseong-gu, Daejeon, 34103, Republic of Korea

[9]Department of Cogno-Mechatronics Engineering, Pusan National University, 2 Busandaehak-ro 63beon-gil, Geumjeong-gu, Busan 46241, Republic of Korea

Demonstration of CHA probes

According to the CHA theory, the reaction of the probe sets for each step was confirmed using gel electrophoretic analysis (Figure S1b). In the absence of the target gene, each probe was stably present without hybridization. However, when the target gene was present, a hybridization chain reaction was observed. In addition, unreacted P^B and P^A-target complex (P^A+T) were also observed at this step, indicating that P^A and the target reacted first to form a complex, followed by the formation of a P^A-P^B complex. P^B aids to increase detection sensitivity by inducing target recirculation and amplification of the fluorescence signal. Their fluorescence intensities were measured every 5 min for 60 min (Figure S2a). In case of P^A and P^B without the target gene, no increase in fluorescence intensity due to nonspecific chain reactions was observed. However, when there was a target gene, the fluorescence intensity increased. Only 1.2 times increase in fluorescence was observed in the reaction with target and P^A alone, whereas a high 1.8 times increase in fluorescence was observed in the reaction with P^A and P^B. Compared to when there was only P^A, the fluorescent signal amplification was increased when the target gene was detected in the probe set in which both P^A and P^B were present, and its fluorescence signal amplification increased gradually with the increase in the concentrations of the target gene. The normalized intensity ($F_{t = 120\ min}$ - $F_{t = 0\ min}$) was linearly dependent on the logarithm (log) of the target concentration in the range of 100 fM-10 nM. The linearly fitted line equation was $y = 155.85x – 252.54$ ($R^2 = 0.9918$). The limit of detection (3.3 σ / slope) was estimated at 1.003 pM (Figure S2b-c). Additionally, when detecting a gene whose target sequence and one or two sequences mismatched (1 sequence mismatch: 1MS and 2 sequence mismatches: 2MS), the fluorescence signal amplification was not sufficient, confirming that the probe sets showed high selectivity and sensitivity of target gene detection (Figure S2d).

The performance of the exoNA sensing hydrogel with in vitro samples

Preferentially, exoNA-sensing hydrogels were tested using mRNA extracted from cells and exosomes (cellular mRNA and exosomal mRNA), respectively. Fluorescence was measured 2 h after cellular mRNA (500 ng in 20 μL) extracted from each cell was dropped onto the detection hydrogels (Figure S13a). HCC1954-treated *ERBB2*-gel showed strong fluorescence and significantly increased fluorescence intensity compared to NTC and HCC1143, while HCC1143 showed a fluorescence signal similar to NTC. In contrast, when the *GAPDH*-gel was treated with cellular mRNA regardless of the cell line, fluorescence signals above the value identified in the NTC-treated *GAPDH*-gel were measured. The detection results of each sensing gel treated with exosomal mRNA (20 ng per 20 μL) were similar to that of cellular mRNA treatment. Similarly, *ERBB2* was only detected in HCC1954 and *GAPDH* was detected in both cells. (Figure S13b).

Experimental section

Reagents, materials, cell lines, and animals: Poly(ethylene glycol) (Mn 3,350) (PEG 3.35K), *N,N*-diisopropylethylamine (DIPEA), dichloromethane (DCM), chloroform, L-α-phosphatidylcholine (PC), 3β-hydroxy-5-cholestene (Cholesterol), 2-hydroxy-2-methylpropiophenone (HMPP) as a radical photo-initiator, 1,2-dioleoyl-3-trimethylammonium-propane (DOTAP), Nile red and Triton X-100 were purchased from Sigma-Aldrich (USA). Acryloyl chloride was purchased from Tokyo Chemical Industry Co. (TCI, Japan). 10×TBE buffer and 1×TE buffer were purchased from Biosesang (Korea). Poly (dimethylsiloxane) Sylgard 184 was purchased from Dow Corning. SU-8 negative photoresist, SU-8 developer was purchased from Microchem (Japan). Acrylamide/bis-acrylamide solution (19:1, 40%), tetramethylethylenediamine (TEMED), and ammonium persulfate (APS) were purchased from Bio-Rad Lab., Inc. (USA). RPMI-1640 medium, Dulbecco′ s Modified Eagle′ s medium (DMEM), fetal bovine serum (FBS), exosome-depleted FBS, 100× penicillin-streptomycin (P/S), BCA protein assay kit, and Ultra-low range DNA ladder were purchased from Thermo Fisher Scientific Inc (USA). Exo-spin™ kit was purchased from Cell Guidance systems (UK). Amicon® ultra centrifugal filter (molecular weight cut-off: 50 K) was purchased from Merck Millipore (USA). ExoRNeasy Maxi kit, RNeasy Mini Kit, miScript II RT kit, and miScript SYBR Green PCR Kit were purchased from Qiagen (Germany).

Synthesis of bioprobes for exoNA detection: Bioprobes were designed to amplify the fluorescence signal through sequential self-cycling in non-enzymatic conditions for highly sensitive detection of exoNA. These were composed of 2 types of bioprobes with hairpin structures (probe A and B), which were activated via nonenzymatic cascade reaction of hairpin probes after the detection of target RNA. To confirm exoNA detection by the FRET effect,

probe A was modified with fluorescein (FAM) at the 5` end and BHQ1 at the 3` end. Before the experiments, each probe was annealed at 90 ℃ for 5 min and cooled down slowly to room temperature for a hairpin structure formation. All the bioprobes were stored at −20 ℃ until use so that the suppression of fluorescence signal was well maintained. All bioprobes and exoNA (*ERBB2* and *GAPDH*) sequences are listed in **Table S1** and were purchased from Bioneer (Korea). In the exoNA detection test using synthetic genes, DNA was used instead of RNA. The cascade reaction of bioprobes enabling fluorescence signal amplification was confirmed using polyacrylamide gel electrophoresis (PAGE) analysis. After loading the probes that serially reacted in each step on the gel, it was run on a 10% acrylamide solution with 1 × TBE buffer under constant voltage (80 V) for 1.5 h at room temperature, and then stained with nucleic acid staining dye (Gel-Red) for 10 min to visually confirm the bioprobe reaction using a gel imaging system (Bio-Rad Laboratories, USA).

Preparation of probe-loaded liposomes: To stably load the probe without nonspecific reactions, each probe was individually loaded into the liposome. First, liposomes were prepared according to the classical thin lipid film hydration method. A total of 7 mg of PC, 0.7 mg of DOTAP, and 1.95 mg of cholesterol were dissolved in 10 mL of chloroform solution. The solution was evaporated using a rotary vacuum evaporator system at room temperature. Subsequently, 1 mL of 10 nM probe in TE buffer solution was added to the lipid film. Then, the solution was vortexed at maximum speed to ensure the detachment of the film from the glass wall of the recipient. For stability, the liposome was stored at 4 ℃ overnight. To eliminate the unloaded free probe, the obtained liposome solution was filtered using Amicon®

ultra centrifugal filter by centrifugation at 4,000 rpm at 4 ℃ for 1 h. The obtained solution was stored at 4 ℃ until use.

Characterization of probe-loaded liposomes: Probe-loaded liposomes were characterized using dynamic light scattering (DLS) (ELSZ-2000, Otsuka). The size of probe-loaded liposome was measured at 10 min intervals for 90 min in various concentrations (0.1, 0.5, 1.0, 2.0 and 5.0 wt%) of Triton X-100 containing 1×TNaK buffer ((20 mM Tris, pH 7.5; 140 mM NaCl; 5 mM KCl) for optimal reaction conditions capable of degrading both liposomes and exosomes. A concentration of 1.0 wt% of Triton X-100 was selected as the optimal reaction buffer (1× TNaK- 1% of Triton in the lysis buffer). In addition, 1 μg of Nile red, a lipid staining dye, was added in the mixed lipid solution to visually confirm the degradation of the probe-loaded liposome.

Preparation of 3D nanostructured hydrogels (exoNA-sensing hydrogel): First, polyethylene glycol diacrylate (PEGDA) was synthesized as a hydrogel backbone according to previously published protocols(Shin et al. 2020). First, 60 g of PEG was completely dissolved in 75 mL of DCM. After this solution became transparent, 7 mL of DIPEA was injected, followed by a dropwise injection of 6.5 mL acryloyl chloride while stirring vigorously on ice. This mixture was stirred overnight under a nitrogen atmosphere with protection from light. Subsequently, this reactant was precipitated in 1 L of diethyl ether and filtered, and the filtrate was vacuum dried to obtain a powder form. To eliminate by-products, the obtained powder was dissolved in 75 mL of DCM and 500 mL 2M potassium carbonate (K_2CO_3) to phase separate the solution overnight. The lower organic solution filtered and precipitated in 1 L of diethyl ether and was

dried under vacuum. Synthesized PEGDA was stored at 4 ℃ until further use. The 3D-nanostructure hydrogels were prepared by photo-polymerization of PEGDA. Cylindrical 3D mass (height: 1 mm, diameter: 8 mm) manufactured by a photo-curing 3D printer was bound on a PDMS mold to form a hydrogel mold. Aqueous solutions containing PEGDA (20 wt %), PEG (20 wt %), probe-loaded liposomes (10 pmol of the probe), and 0.1 % (w/v) HMPP were poured into this mold and then photo-polymerized using an UV lamp at a wavelength of 365 nm for 2 min. The fabricated 3D-nanostructure hydrogels were rinsed in DW for 2 h and dried overnight at room temperature. After the hydrogels were completely dry, these hydrogels were also stored at 4 ℃ until use.

Characterization of exoNA-sensing hydrogel: Hydrogels were allowed to hydrate in TE buffer overnight. The gel samples were then frozen in a −80 °C refrigerator for 24 h and lyophilized for 2 days to fully remove the water. The samples were then preserved at 4 °C under nitrogen gas until imaging. SEM images were taken using a JEOL SEM (JSM-IT800), and the gels were cut with a razor blade, sputter-coated with gold to enhance contrast and imaged on the cross-section. cryo-SEM images were taken using ZEISS crossbeam 550 (FIB-SEM). The samples were first mounted on a cryo-SEM sample holder, and then plunged into a freezing liquid ethane bath and then transferred to a liquid nitrogen bath. Once cooled down both sample holder and specimen were transferred to a protected atmosphere shuttle under low temperature and vacuum conditions to prevent contamination. cryo-SEM sample preparation system in order to expose a fracture profile of the network by impacting the cross section of the specimen with a blade. Finally, the specimen was transferred via the same shuttle to the pre-cooled SEM chamber to be imaged.

Fabrication of the exoNA-sensing chip: The microfluidic channel was fabricated by attaching the PDMS microchannel on a slide glass. For complete adhesion, O_2 plasma treatment was applied on both surfaces. Before microchannel adhesion, synthesized hydrogels were located on a slide glass. The PDMS-based microchannel was made from SU-8 master mold by casting, followed by thermal curing. The mixture of base and curing agent (10:1 weight ratio) was poured onto the SU-8 master mold and heated at 80 ℃ for 6 h. Microfluidic channel patterns were obtained through a simple photolithography process using SU-8. SU-8, an epoxy-based negative photoresist, were spin coated onto Si waters with a thickness of 10 μm. To prevent unexpected adhesion on the inner surface of the microfluidic channel, self-assembled monolayers (SAMs) were employed.

Cell culture: Breast cancer cell lines, HCC1954 (ATCC® CRL-2338™), HCC1143 (ATCC® CRL-2321™), MCF7 (ATCC® HTB-22™), SK-BR-3 (ATCC® HTB-30™), and MDA-MB-231 (ATCC® HTB-26™), were purchased from American Type Culture Collection (ATCC, USA). HCC1954, HCC1143, SK-BR-3 cell lines were cultured in RPMI-1640 medium supplemented with 10% FBS 1× penicillin-streptomycin. MCF7 and MDA-MB-231 cell lines were cultured in DMEM containing 10% FBS and 1× P/S.

Orthotopic HER2-positive breast cancer animal model: All animal experiments were conducted with the approval of the Institutional Animal Care and Use Committee of the Yonsei Laboratory Animal Center (IACUC 2017–0329). Female BALB/c nude mice of age 4~6 weeks (n = 5, average weight 21 ± 6 g) were purchased from Central Lab Animal Inc (Seoul, Korea). After a week of acclimatization, each mouse was housed in individual cages under an automatically controlled air condition system at a particular temperature (22 ± 2 °C), humidity

(approximatly 60%), and light conditions (12:12-h light–dark cycle). Diet (Pico Lab 5053, LabDiet, CA, USA) and sterilized water were provided ad libitum throughout the experiments. HCC1954 cells were injected with 60 μL containing 6 $\times 10^6$ cells suspended in serum-free media into the mammary fat pad of mice using insulin syringe (29G). After cancer cell implantation, mice were monitored until the tumor volume expanded up to 1,000 mm^3 or was ulcerated. The implanted tumor sizes were measured three times per week, and each volume was calculated by equation (1).

$$Tumor\ volume\ (mm^3) = \frac{4}{3} \times \pi \times \left(\frac{Minor\ axis}{2}\right)^2 \times \left(\frac{Major\ axis}{2}\right)^2 \quad \cdots\cdots\ Equation\ (1)$$

Exosome isolation: Each breast cancer cell was cultured in an exosome-free medium (containing 10% exosome-depleted FBS) for 48 h. After collecting the conditioned medium, cellular debris was eliminated using centrifugation at 300 × *g* for 10 min and filtered through a 0.45μm syringe filter (Millipore). Next, in order to collect exosomes, an equal volume of Exo-spin^{TM} buffer was added, as a sample, to purified media, and incubated at 4 ℃ for 2 h.

Mixed solutions were concentrated by centrifugation at 16,000 × g for 60 min and subsequently, the supernatant was discarded carefully. Concentrated exosomes were re-suspended in 100 μL of TNaK buffer. Blood samples from HER2-positive tumor-bearing mice were collected and centrifuged at 1,500 × *g* for 15 min to transfer plasma, followed by centrifugation at 16,000 × *g* for 30 min to remove residual cell debris. The fresh plasma was obtained by filtering the sample through a 0.45 μm filter. The procedure of isolating exosomes in plasma was performed in the same manner as for cells.

Characterization of exosome: For particle size and number determination, nanoparticle tracking analysis (NTA) was performed with a NanoSight NS300 instrument equipped with

the NTA software. All experiments were carried out at 1:1,000 dilution, leading to particle concentrations around 3×10^{10} mL^{-1}.

TEM imaging: The isolated exosome sample was fixed 1:1 with 2% glutaraldehyde (v/v; Sigma Aldrich, Saint Louis, MO) for 30 min. A fixed sample was pipetted onto a 200-mesh copper grid with carbon-coated formvar film, and incubated for 10 min. Excess liquid was removed by blotting. The grid was washed twice by brief contact with 100 µL MilliQ water, followed by blotting to remove excess liquid. JEOL 1010 TEM was used to image exosome samples at a voltage of 80 kV.

qRT-PCR: Cellular mRNA was extracted using the RNeasy Mini Kit (Qiagen, Germany), and exosomal mRNA in the cell culture medium and plasma were extracted using the exoRNeasy Maxi kit (Qiagen, Germany). The concentration of extracted mRNA was measured using the Nanodrop™ 2000 (Thermo). For analysis of mRNA expression levels, extracted mRNA was reverse-transcribed to generate first-strand cDNA (miScript II RT kit, Qiagen) and real-time PCR detection of cDNA was performed using a CFX96™ Real-Time PCR detection system (Bio-rad) according to the protocol of miScript SYBR Green PCR Kit. All experiments were performed in triplicate and relative quantification was calculated for each sample by normalizing it with the corresponding *GAPDH* expression. The sequences of the primers are summarized in **Table S3**.

Western blotting: Exosomes were lysed in radioimmunoprecipitation assay (RIPA) buffer (Thermo Fisher Scientific) and protein concentrations in the exosomes were measured by the bicinchoninic acid assay (BCA assay, Thermo Scientific). Protein lysates were separated by sodium dodecyl sulfate polyacrylamide gel electrophoresis (SDS–PAGE), transferred to a

polyvinylidene fluoride membrane (PVDF, Invitrogen), and immunoblotted with the corresponding antibodies of each protein (CD9; ab2215, Abcam, CD81; ab59477, Abcam, GAPDH; ab8245, Abcam). All the antibodies were used at a 1,000-fold dilution. Following incubation with horseradish peroxidase (HRP)-conjugated secondary antibody, chemiluminescence was used for immunodetection (Thermo Scientific).

***Fluorescence measurement*:** The fluorescence intensity of probes was observed with a fixed gain (λ_{ex} = 484 nm and λ_{em} = 530 nm) and performed on a Cytation 5 plate reader (BioTek). The increase in fluorescence intensity of probes before and after treatment with the target gene was measured. Both probes (50 μL) were mixed, and its fluorescence intensity (F_0) was measured prior to treatment with the target gene. Next, 1 μL of target gene (100 fM to 100 nM) was added into the probes solution and measured at 10 min intervals for 2 h (F).

ExoNA detection using exoNA-sensing hydrogels: The 3D-nanostructured hydrogels were incubated with 20 μL of a sample containing TNaK buffer (1% of Triton X-100) for 120 min. Various concentrations (62.5 fmol to 1 pmol) of target genes, synthetic genes, and exosomal mRNAs extracted from cells, cultured media, or tissues of animal models, were treated on the 3D-nanostructured hydrogels. The fluorescence intensity was measured with the gel imaging system (Bio-Rad Laboratories, USA).

ExoNA detection using the exoNA-sensing chip: Before testing, the inlet and outlet of the exoNA-sensing chip were blocked, and the inside was maintained at a vacuum state through a degassing process for 30 min using a vacuum chamber. Approximately 100 μL of a sample solution was injected into the inlet and allowed to react for 2 h at room temperature, and then

fluorescence of the sensing parts was measured using the gel imaging system (Bio-Rad Laboratories, USA).

Data analysis and statistics: Data have been obtained by using at least three independent experiments. The exact number of replicates has been inserted in each graph. Data have been reported as mean (m) ± SD. The following legend has been added to the figures: **p*-value < 0.05; ***p*-value < 0.005; and ****p*-value < 0.00005. LOD was calculated using the following equation: LOD = 3σ/m, where σ is the SD of blank and m is the slope of linear fitting of data in the linear range.

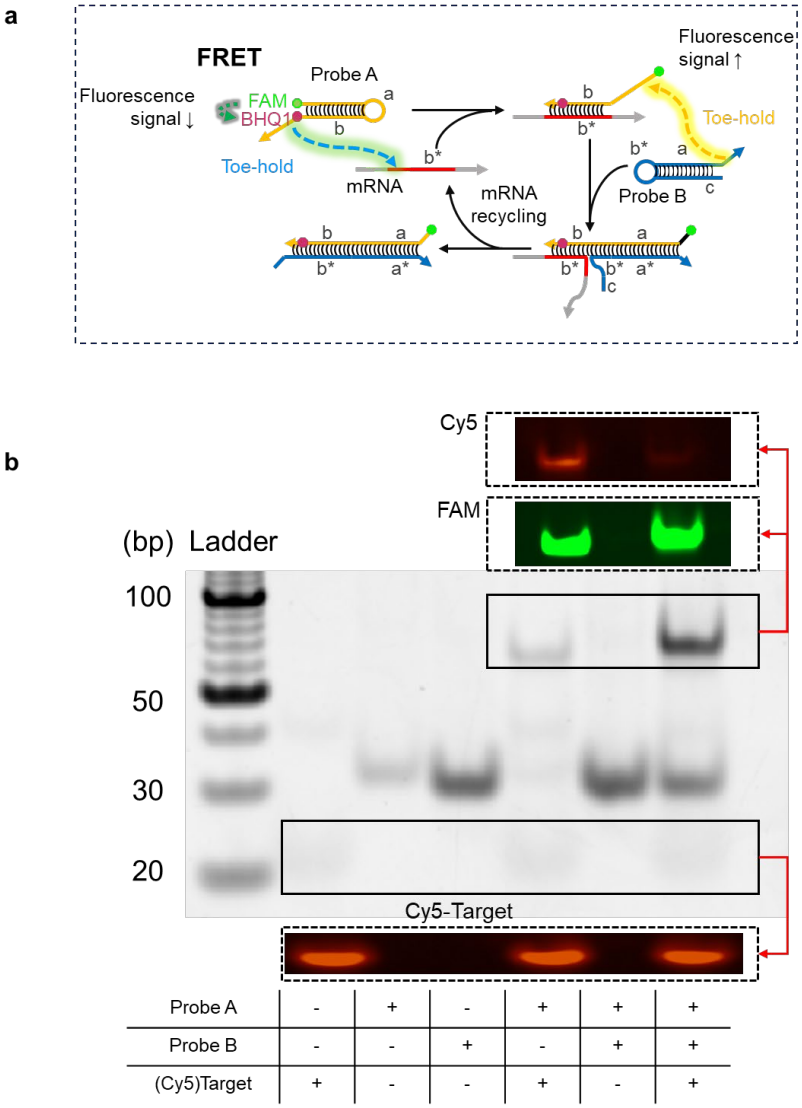

Figure S1. (a) Schematic of isothermal enzyme-free signal amplification by catalytic hairpin assembly-based probe sets for detecting target mRNA with high-sensitivity, and (b) gel electrophoresis analysis of the reaction of the probe and target at each step of the signal amplification reaction at 25°C (+, presence of; -, absence of)

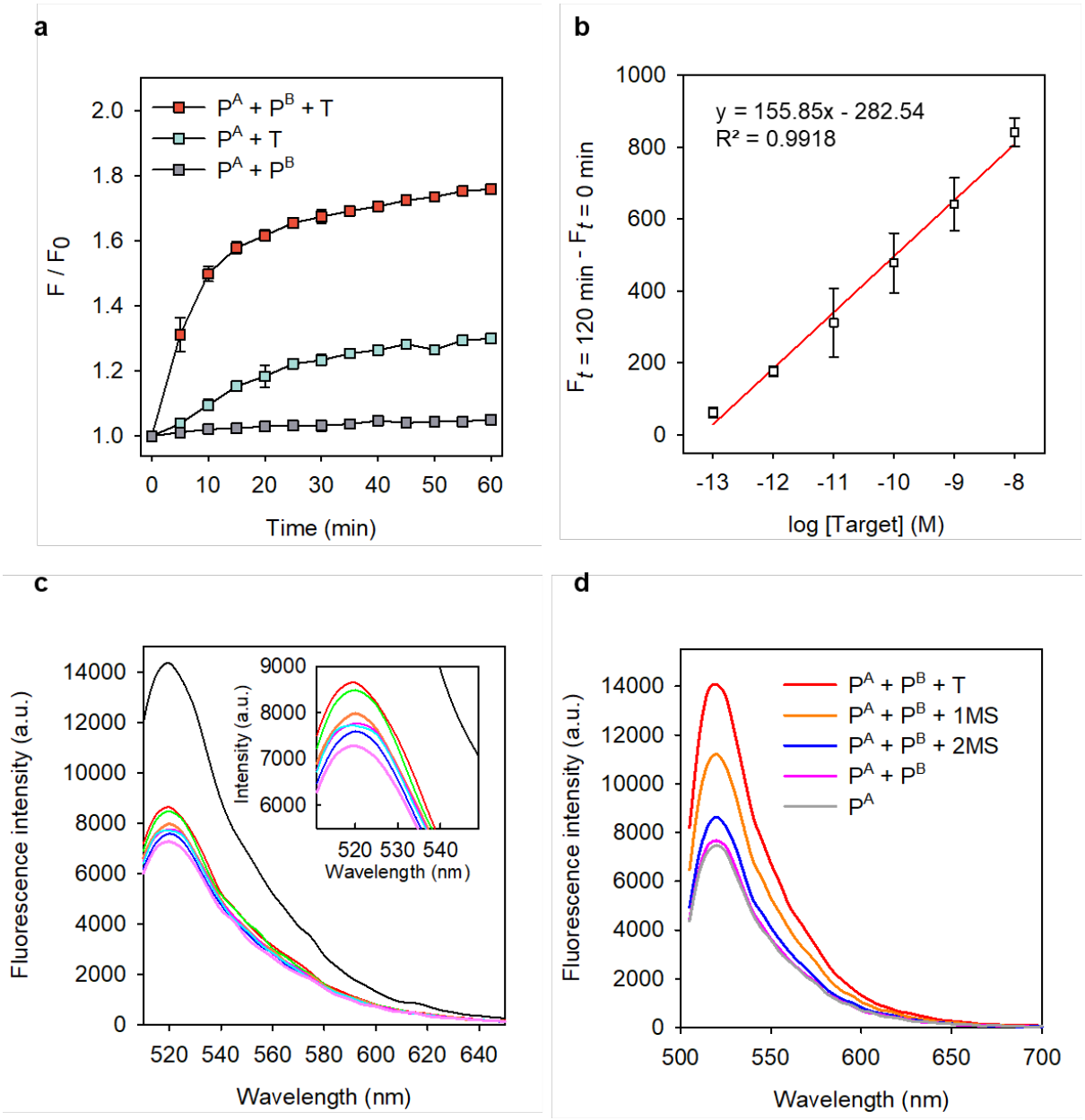

Figure S2. (a) Time response of fluorescence intensity of targets containing P^A, $P^A + P^B$, and $P^A + P^B$ without the target. The target gene (1 nM) was added to each probe solution. (F: fluorescence intensity and F_0: fluorescence intensity at 0 min). (b) The detection sensitivity of target gene concentrations using probe set P^A+P^B by measuring before (t = 0) and after (t = 120 min) treatment with various concentrations of mRNA. Their limits of detection were calculated. (c) The fluorescence spectra of probes set at 120 min after treatment with various target gene

concentrations (black, 100 nM; red, 10 nM; green, 1 nM; orange: 100 pM; purple, 10 pM; cyan, 1 pM; blue, 100 fM; pink, 0 M). (d) The fluorescence spectra of P^A+P^B after treatment with 1 nM of T, 1MS, or 2MS. (T, target gene, 1MS, 1 bp mismatch, 2MS, 2 bp mismatch). Only P^A+P^B and P^A were measured as controls.

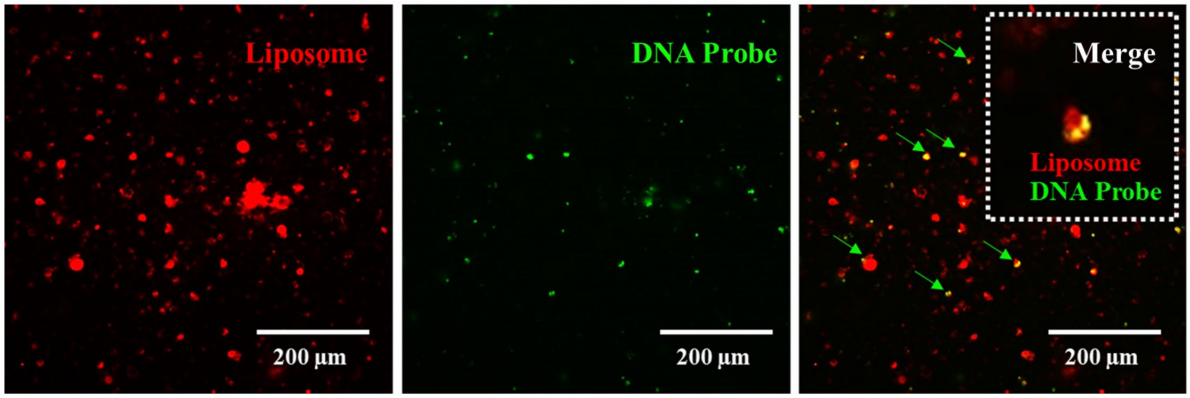

Figure S3. Fluorescence images of probe-loaded liposomes. A lipophilic dye (Nile red) was used to stain the lipid membrane, and fluorophore was used at the 5′ ends of the modified DNA probes. Red and green fluorescence indicate liposome and probe, respectively (left and middle image). The right image is a merge of the left and middle images.

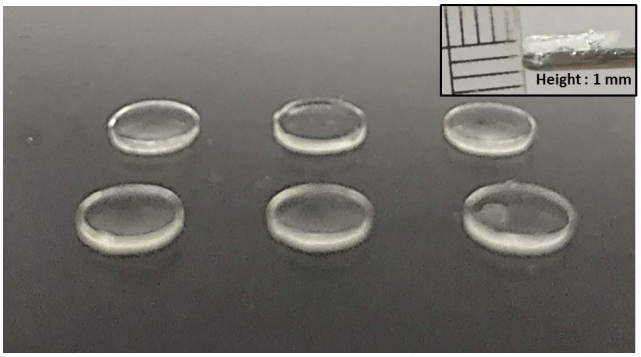

Figure S4. Images of 3D-nanostructure hydrogels. The insert image shows the height of this hydrogel was 1 mm.

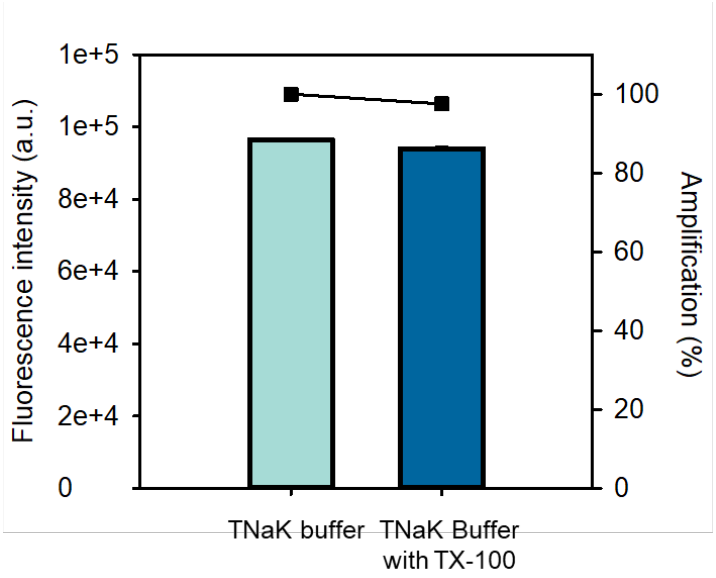

Figure S5. Fluorescence intensity of probes set by catalytic hairpin assembly reaction and their amplification efficiency in 1 wt% $T_{x\text{-}100}$-containing buffer (reaction buffer). Fluorescence intensity was measured 2 h after treatment with target mRNA in each buffer containing probe sets (P^A and P^B), and the amplification efficiency of probe sets in reaction buffer was calculated based on fluorescence intensity in TNaK buffer at 100% (amplification (%) = fluorescence $intensity_{in\ buffer+Tx\text{-}100}$ / fluorescence $intensity_{in\ buffer}$ × 100).

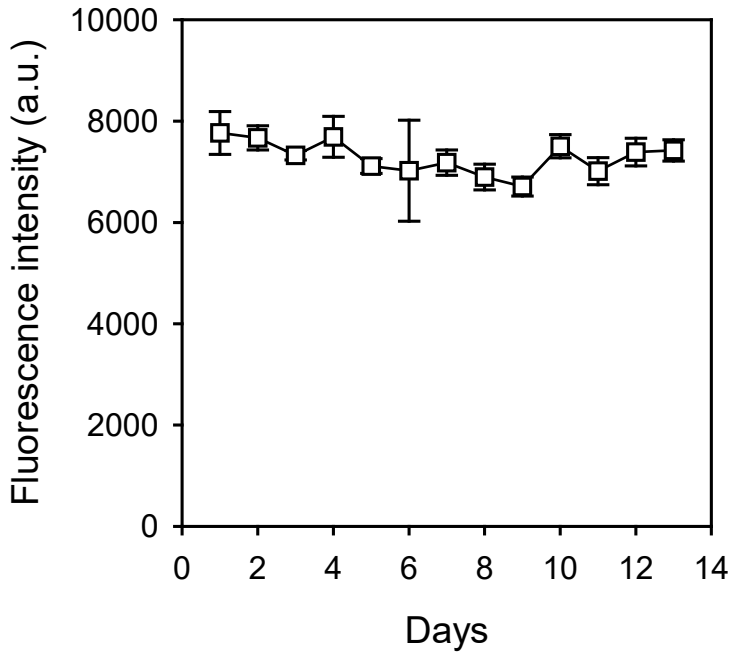

Figure S6. Stability test of exoNA-sensing hydrogel. The fluorescence intensity of exoNA-sensing hydrogel was measured for 13 days.

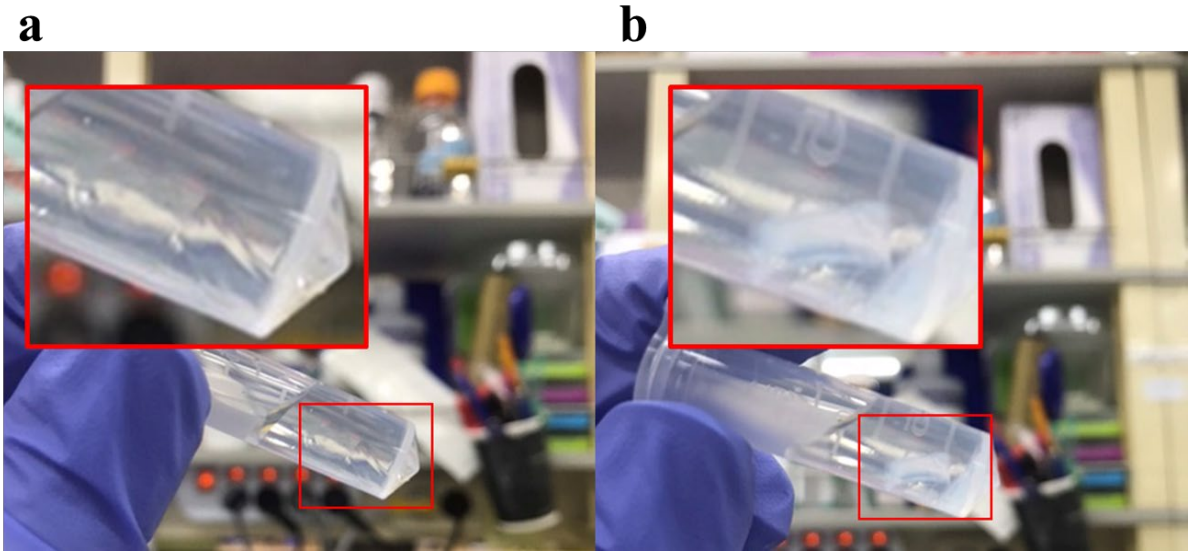

Figure S7. Comparison of porosity of hydrogels. Polyethylene glycol (PEG) serves as a pore in the hydrogels. Images of (a) PEG-free hydrogel and (b) 20 wt% PEG-containing hydrogel. PEG-free hydrogel has no pores and is transparent, and 20 wt% PEG-containing hydrogel has pores and is translucent.

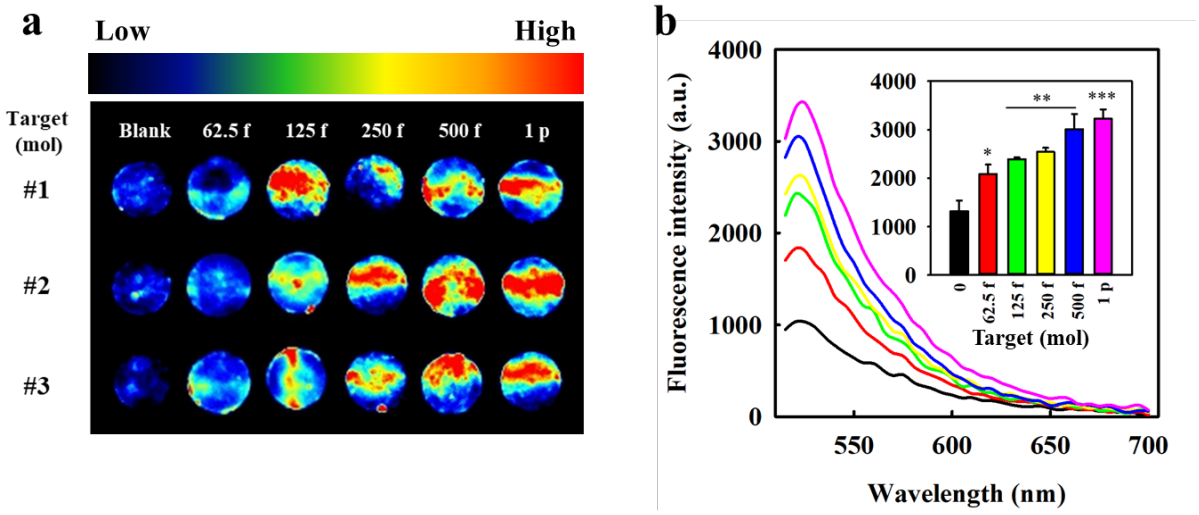

Figure S8. (a) Fluorescence images of exoNA-sensing hydrogels after treatment with various concentrations of target genes (20 μL) (62.5 fmol to 1 pmol) and (b) their fluorescence spectra (purple, 1 pmol; blue, 500 fmol; yellow, 250 fmol; green, 125 fmol; red, 62.5 fmol; black, no template control). The inset bar graph represents the average fluorescence intensity of exoNA-sensing hydrogels measured in triplicate tests. Error bars indicate standard deviation.

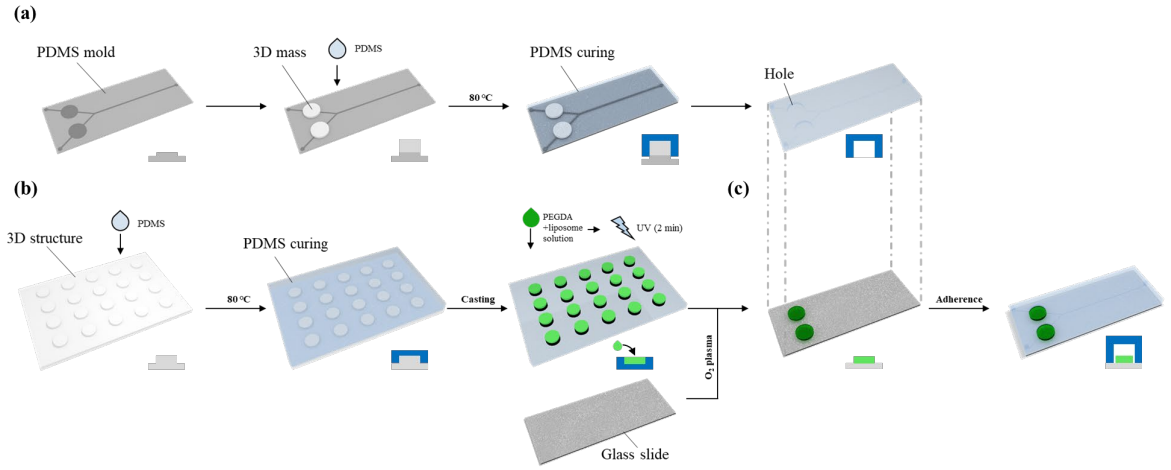

Figure S9. Schematic illustration of the fabrication procedure of exoNA-sensing chip fabrication. Stepwise fabrication of (a) the microfluidic chip using Sylgard 184 silicone elastomer, (b) exoNA-sensing hydrogels, and (c) exoNA-sensing chip.

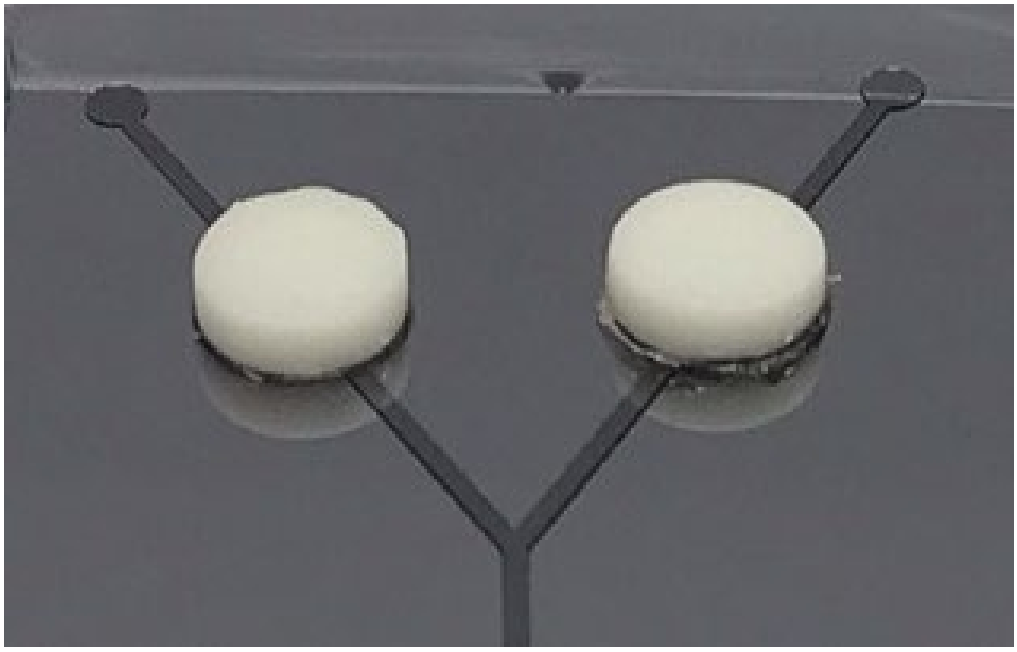

Figure S10. 3D masses were used to make the sensing parts for the exoNA-sensing hydrogel loading chip.

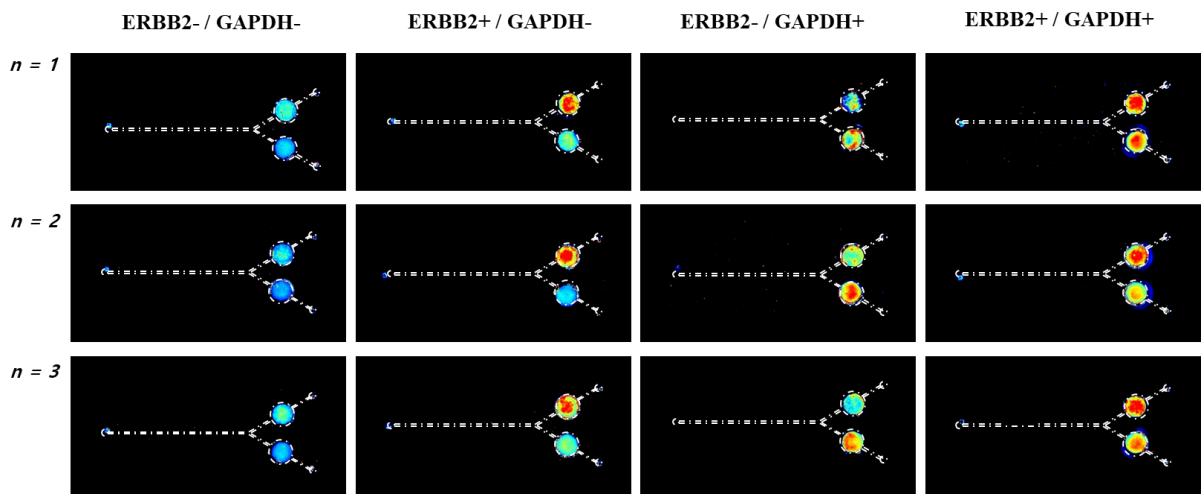

Figure S11. The performance evaluation of the exoNA-sensing chip (top: ERBB2-gel and bottom: GAPDH-gel). The fluorescence image of the exoNA-sensing chip after injection with various target gene mixtures (100 nM) (ERBB2-/GAPDH-, the absence of both genes; ERBB2+/GAPDH-, the presence of ERBB2 and absence of GAPDH; ERBB2-/GAPDH+, the absence of ERBB2 and presence of GAPDH; ERBB2+/GAPDH+, the presence of both genes).

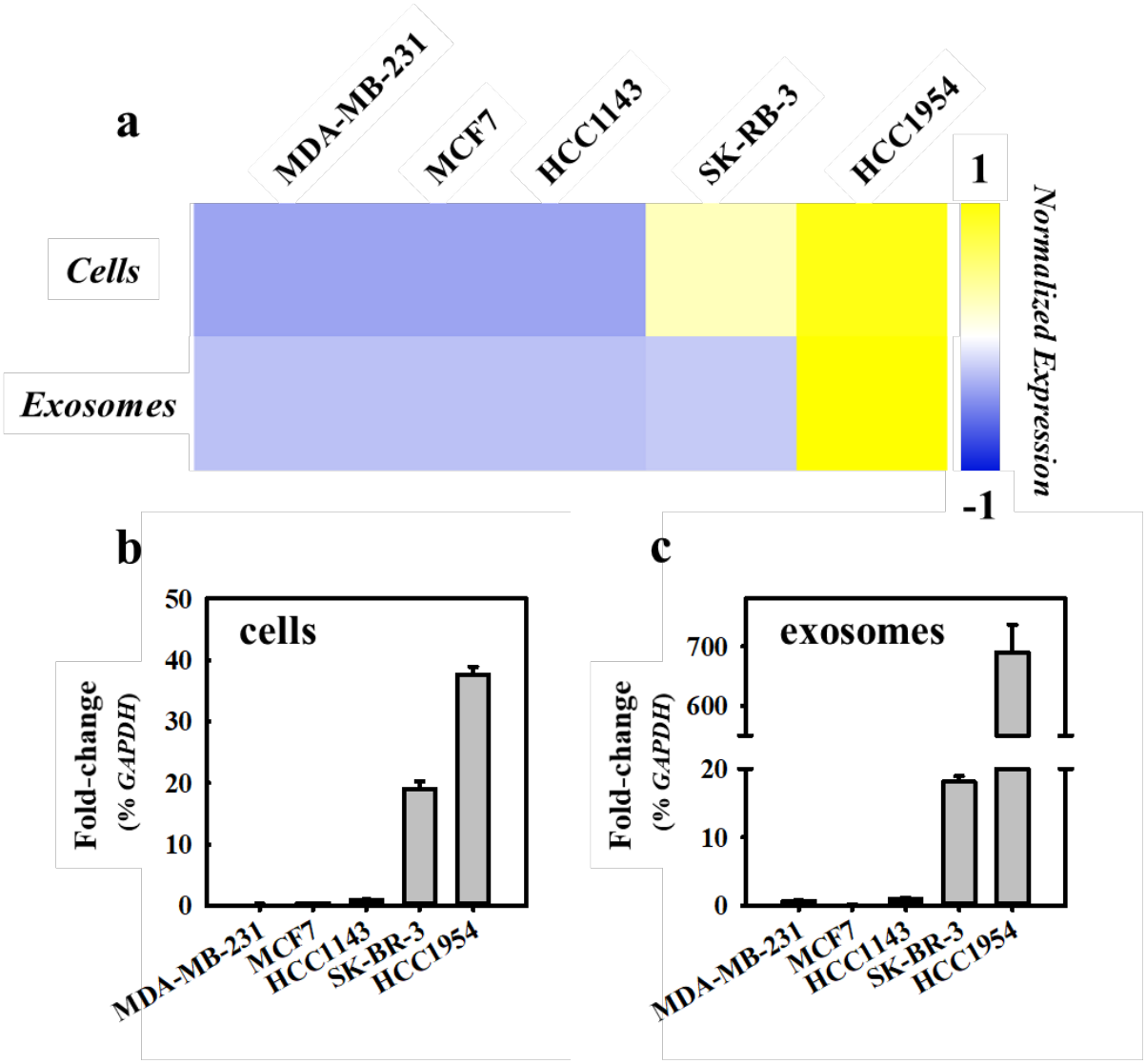

Figure S12. Cellular and exosomal mRNA analysis using qRT-PCR. (a) Heatmap plot of ERBB2 expression levels from cellular and exosomal RNA of five breast cancer cell lines (HER2-negative, MDA-MB-231, MCF7, and HCC1143; HER2-positive, SK-BR-3 and HCC1954). Bar graphs show the comparison of expression levels of ERBB2 derived from (b) cellular and (c) exosomal RNA. The result of qRT-PCR was compared to HCC1143 as the control and normalized by GAPDH as a reference.

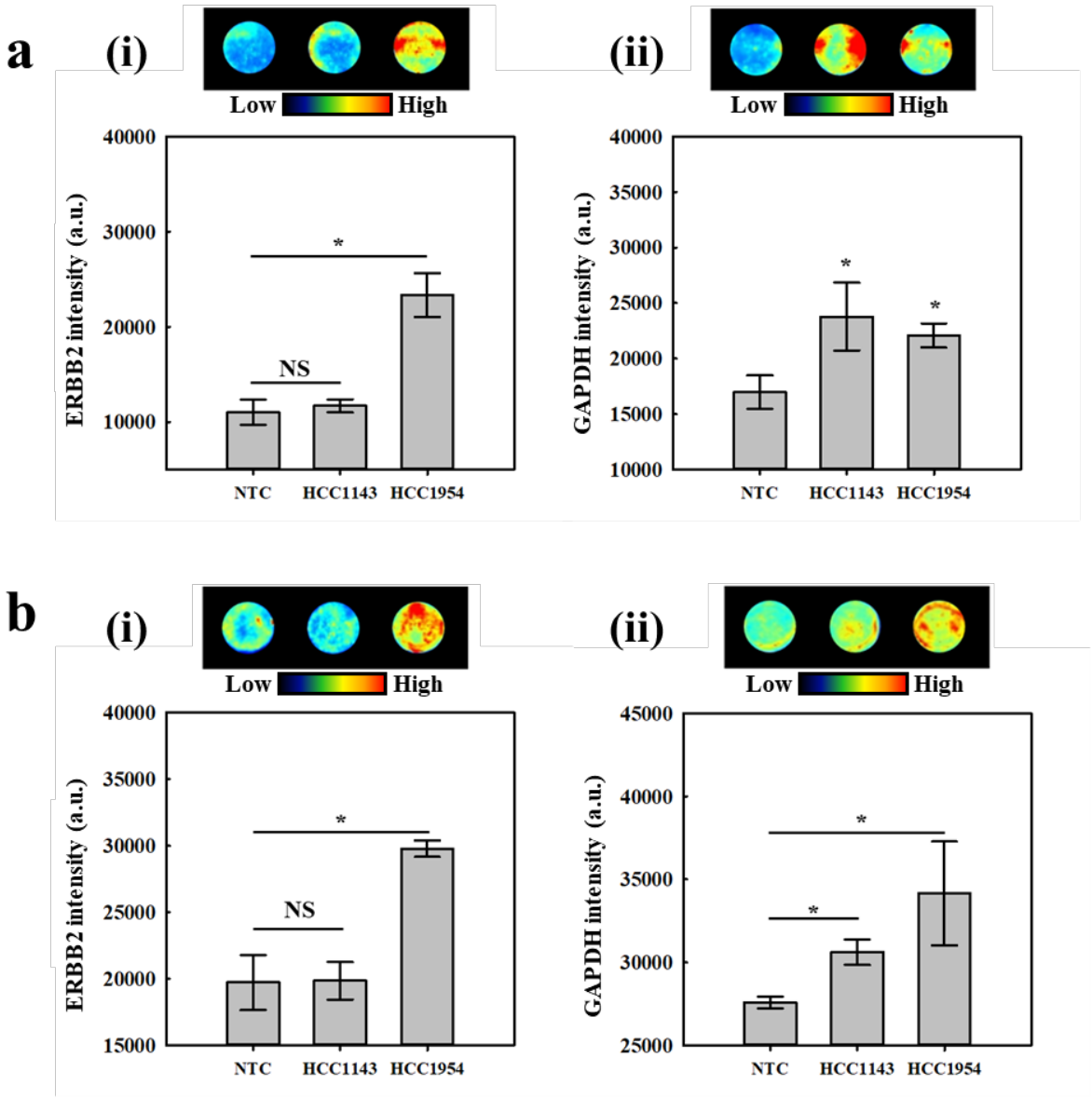

Figure S13. Exosomal RNA analysis using exoNA-sensing hydrogel. (a) The fluorescence image of 500 ng of mRNA isolated from HCC1954 and HCC1143 cells treated on hydrogel (n = 3). The top images show relative fluorescence of (i) ERBB2-gel and (ii) GAPDH-gel. The fluorescence image of 15 ng of exosomal RNA isolated from HCC1954 and HCC1143 cell culture media treated on hydrogel (n = 3).

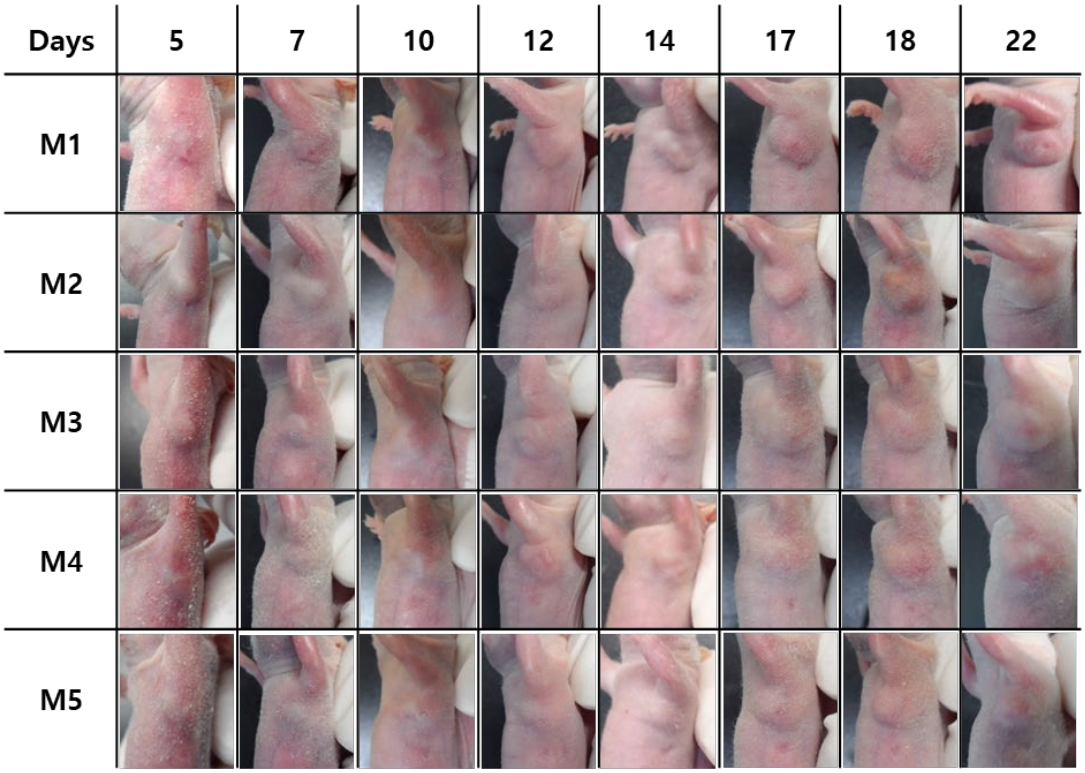

Figure S14. *In vivo* modeling of orthotopic breast tumor by transplanting HCC1954 cells into the mammary fat pad of mice. Images of tumor growth for 22 days after modeling HER2-positive tumor-bearing mice.

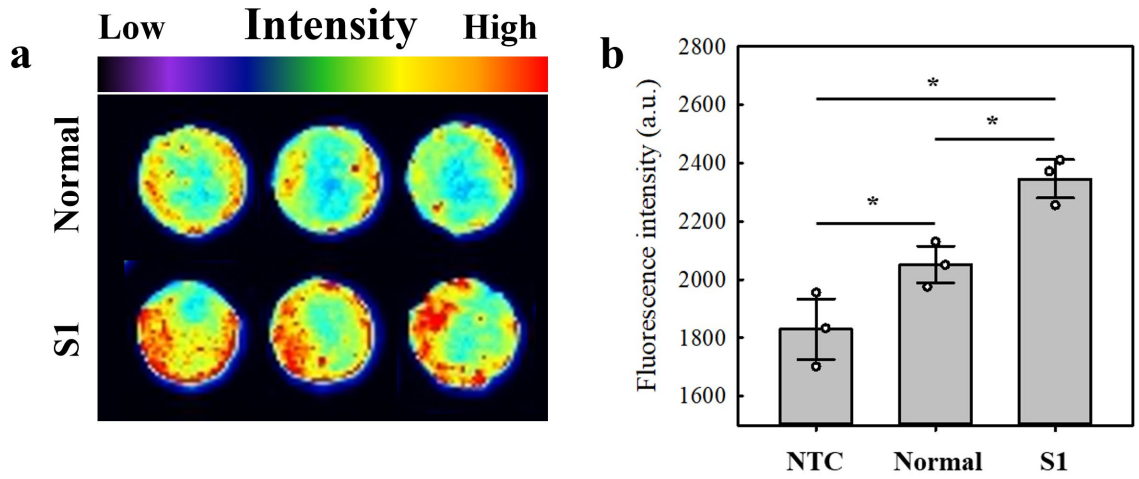

Figure S15. Detection ability of ERBB2-gels using *in vivo* sample (blood). (a) The fluorescence image of ERBB2-gel treated with 500 ng of mRNA isolated from tissue of S1 mice and normal mice ($n = 3$), and (b) their fluorescence intensities (NTC, no template control).

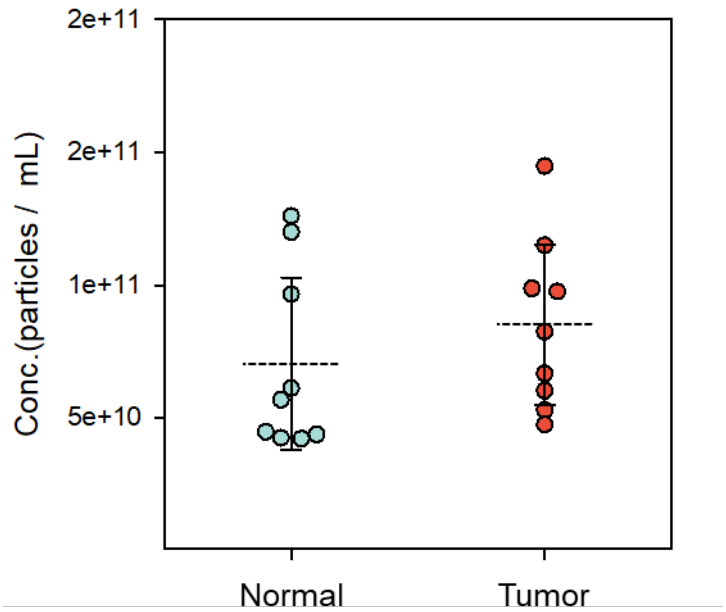

Figure S16. Quantification of exosomes isolated from mouse plasma (n = 9).

a **Normal mouse plasma**

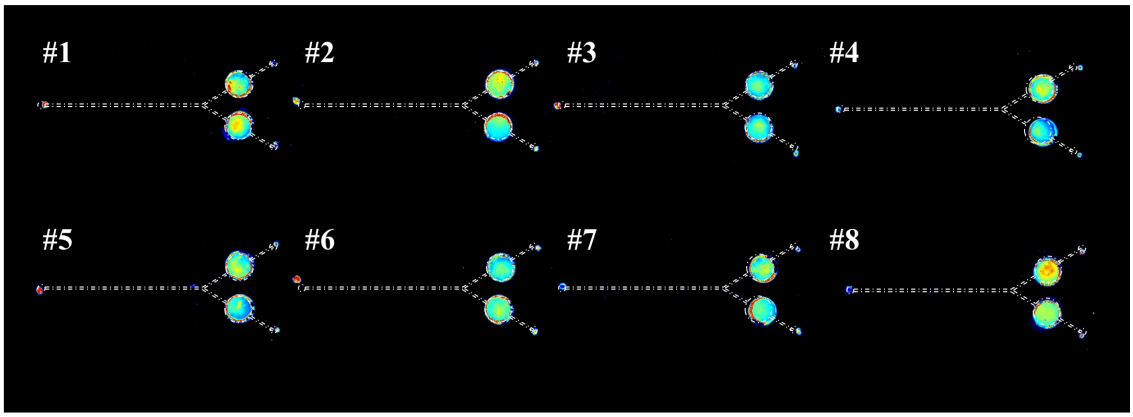

b **S1 phase mouse plasma**

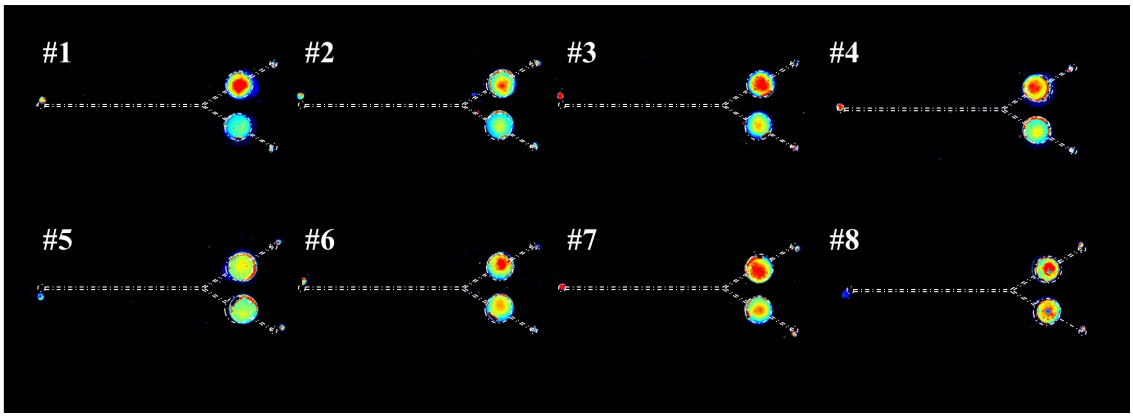

Figure S17. Fluorescence images of the exoNA-sensing chip after injecting exosome samples from the plasma of (a) S1 phase of orthotopic mice and (b) normal mice (n = 8).

Video S1.mov

Video S1. The fluid behavior in the exoNA-sensing chip by vacuum-driven, power-free, micro-pumping process.

Table S1. Sequence information for probes used.

Name	Sequences of oligonucleotide (5′-3′)
A-ERBB2	(FAM)AAA GCG ACC CAT TCA GGC ACC GAG AAC AAA AGC TGA ATG GGT CGC TTT T(BHQ1)GT TCT
B-ERBB2	TCA GGC ACC GAG AAC AAA AGC GAC CCA TTC AGC TTT TGT TCT CGG TGC CTG AAT GGG T
A-GAPDH_*human*	(FAM)GTG AAG GTC GGA GTC AGT TAG TGG GAA GGT GAT GAC TCC GAC CTT CAC CT(BHQ1)T CCC
B-GAPDH_*human*	GTC AGT TAG TGG GAA GGT GAA GGT CGG AGT CAT CAC CTT CCC ACT AAC TGA CTC CGA C
A-GAPDH_*mouse*	(FAM)ACA GCA ACT CCC ACT CGA TAG TGG TTC AAC AGG AGT GGG AGT TGC TGT T(BHQ1)GA AGT
B-GAPDH_*mouse*	ACT CGA TAG TGG TTC AAC AGC AAC TCC CAC TCC TGT TGA ACC ACT ATC GAG TGG GAG T
***T-ERBB2**	TAA GAA CAA AAG CGA CCC ATT CAG
****1MS-ERBB2**	TAA GAA CAA AA***C*** CGA CCC ATT CAG
*****2MS-ERBB2**	TAA GA***T*** CAA AA***T*** CGA CCC ATT CAG
T-GAPDH_*human*	TGG GGA AGG TGA AGG TCG GAG TCA
1MS-GAPDH_*human*	TGG GGA AG***C*** TGA AGG TCG GAG TCA
2MS-GAPDH_*human*	TG***C*** GGA AG***C*** TGA AGG TCG GAG TCA
T-GAPDH_*mouse*	CGA CTT CAA CAG CAA CTC CCA CTC

*T, Target gene sequence, **1MS,1 base mismatched sequence, ***2MS, 2 base mismatched sequence, ******Italic***, mismatched base

Table S2. Relative mRNA expression levels in (a) breast cancer cell lines and (b) exosomes secreted by each cell line analyzed using qRT-PCR.

Cell lines	HCC1143	MDA-MB-231	MCF7	SK-BR-3	HCC1954
(a) Cellular mRNA					
ERBB2	1.00 ± 0.06	0.33 ± 0.04	0.42 ± 0.02	19.04 ± 1.23	37.68 ± 1.26
(b) Exosomal mRNA					
ERBB2	1.00 ± 0.16	0.75 ± 0.06	0.19 ± 0.01	18.10 ± 0.85	690.14 ± 46.45

Relative expression ± SEM
The ΔCt values were normalized by GAPDH, and ΔΔCt values were calculated by HCC1143 (HER2-negative cell line).
*The relative expression level was calculated by $2^{-\Delta\Delta Ct}$.
*SEM is standard error of the mean.

Supplementary Table 3. Sequence information for PCR primers used.

Name	Sequences of oligonucleotide (5'-3')
PPP1R1B_*F*	ATC CTC ACC CTG TTT TGT GC
PPP1R1B_*R*	CGG TTT TCT GGA TTT TCC AAT
STARD3_*F*	GGT CTG GCC TGT TGA TGT TTA
STARD3_*R*	GAA GAG CCC CTT CAT CTT CAC
ERBB2_*F*	CTC GTT GGA AGA GGA ACA GC
ERBB2_*R*	CTG AAT GGG TCG CTT TTG TT
GRB7_*F*	AGT CCA CTC CTG ACC CCT CT
GRB7-*R*	AAC TGG CCT CTC GGT CTG TA
GAPDH_*F*	GCT CTC TGC TCC TCC TGT TC
GAPDH_*R*	TGA CTC CGA CCT TCA CCT TC